

# Variability of FP-CIT PET Patterns Associated With Clinical Features of Multiple System Atrophy

Reeree Lee, MD,\* Jung Hwan Shin, MD, PhD,\* Hongyoon Choi, MD, PhD, Han-Joon Kim, MD, PhD, Gi Jeong Cheon, MD, PhD, and Beomseok Jeon, MD, PhD

*Neurology*® 2021;96:e1663-e1671. doi:10.1212/WNL.00000000000011634

## Correspondence

Dr. Choi  
chy1000@snu.ac.kr  
or Dr. Kim  
movement@snu.ac.kr

## Abstract

### Objective

To validate the role of the dopamine transporter (DAT) imaging as a biomarker in multiple system atrophy (MSA), we analyzed the association between spatial patterns of [ $^{18}\text{F}$ ]fluoropropyl-carbomethoxy-iodophenyl-tropane ([ $^{18}\text{F}$ ]FP-CIT) PET and the clinical characteristics of MSA.

### Methods

Sixty-five patients with MSA who underwent [ $^{18}\text{F}$ ]FP-CIT PET between 2009 and 2018 were retrospectively enrolled. To identify spatial patterns of [ $^{18}\text{F}$ ]FP-CIT PET, principal component (PC) analysis was used and correlated with the clinical presentation.

### Results

Of the 65 patients, 42 presented with parkinsonian subtype of MSA, and 23 presented with cerebellar subtype of MSA (mean age  $63.7 \pm 9.3$  years; disease duration,  $1.8 \pm 1.8$  years). Each PC represents a specific pattern of degeneration: PC1 and PC2 were associated with the DAT binding of the entire putamen and the posterior putamen, respectively. PC3 was associated with increased [ $^{18}\text{F}$ ]FP-CIT uptake of the caudate and decreased uptake of the dorsal pons. PC2 was significantly correlated with the presence of parkinsonism ( $p = 5.34 \times 10^{-5}$ ) and a positive levodopa response ( $p = 0.044$ ), with age as a cofactor. PC3 was correlated with the presence of urinary incontinence ( $p = 0.036$ ). Onset age was significantly correlated with both PC2 ( $R = 0.48$ ,  $p = 5.0 \times 10^{-5}$ ) and PC3 ( $R = -0.39$ ,  $p = 0.0013$ ).

### Conclusions

The spatial pattern of DAT binding can reflect distinct clinical features of MSA and provides insight into the underlying pathophysiology of a broad spectrum of clinical features in MSA.

\*These authors contributed equally to this work.

From the Department of Nuclear Medicine (R.R.), Chung-Ang University Hospital, and Departments of Neurology (J.H.S., H.-J.K., B.J.), and Nuclear Medicine (H.C., G.J.C.), Seoul National University Hospital, Korea.

Go to [Neurology.org/N](https://www.neurology.org/N) for full disclosures. Funding information and disclosures deemed relevant by the authors, if any, are provided at the end of the article.

## Glossary

BR = binding ratio; DAT = dopamine transporter; DRPLA = dentatorubral-pallidoluysian atrophy; [ $^{18}\text{F}$ ]FP-CIT = [ $^{18}\text{F}$ ] fluoro-propyl-carbomethoxy-iodophenyl-tropane; MSA = multiple system atrophy; MSA-C = cerebellar subtype of MSA; MSA-P = parkinsonian subtype of MSA; PAG = periaqueductal gray; PC = principal component; SCA = spinocerebellar ataxia.

The clinicopathologic correlation of multiple system atrophy (MSA) can be characterized as a combination of presynaptic (nigral) and postsynaptic (striatal) neurodegeneration for parkinsonism, pontocerebellar degeneration for cerebellar ataxia, and the degeneration of extrastriatal structures such as the brainstem nucleus, which is related to sleep apnea and respiratory dysfunction.<sup>1</sup> Thus, evaluation of neurodegeneration in the striatum and extrastriatal structures is required to interrogate the overall pathophysiology of MSA.

The dopamine transporter (DAT) PET radiotracer [ $^{18}\text{F}$ ] fluoro-propyl-carbomethoxy-iodophenyl-tropane ligand ([ $^{18}\text{F}$ ] FP-CIT) not only binds to the DAT in the striatum but also partly binds to the serotonin noradrenergic transporter, which is rich in brainstem nuclei.<sup>2</sup> The spatial pattern of neurodegeneration in striatal and extrastriatal structures may reflect various clinical features of MSA and provide a better understanding of the pathophysiology. Previous studies have shown that the DAT binding in MSA was different from that in other parkinsonian syndromes<sup>3</sup> and between MSA subtypes.<sup>4</sup> However, the association between DAT imaging patterns and the clinical features of MSA has not been clearly elucidated.

Currently, the pathophysiology of MSA is based on autopsy findings, which are limited in their application to live patients. Therefore, in vivo biomarkers associated with the clinical symptoms of MSA are crucial because they could be used to elucidate the clinicopathologic correlates of the underlying neurodegeneration. We analyzed the spatial pattern of [ $^{18}\text{F}$ ] FP-CIT PET in patients with clinically diagnosed MSA with a voxel-wise and data-driven method. Accordingly, we extracted spatial patterns of neurodegeneration on PET and then examined their associations with the clinical features of MSA.

## Methods

### Patients

We retrospectively reviewed the medical records of patients who were diagnosed with clinically probable/possible MSA according to the second consensus criteria<sup>5</sup> and underwent [ $^{18}\text{F}$ ]FP-CIT brain PET between January 2009 and December 2018. For clinical information, we assessed age, sex, onset of motor symptoms, and date of [ $^{18}\text{F}$ ]FP-CIT PET. Clinical signs of parkinsonism (bradykinesia, rigidity, and tremor), cerebellar dysfunction (ataxia, dysarthria, and ocular dysfunction), and autonomic dysfunction (orthostatic hypotension, urinary dysfunction, and erectile dysfunction) were reviewed. The patients were routinely followed up every 1 to 3

months at the clinic, and the diagnosis was reappraised at every visit. For exclusion of MSA-mimic disease, we performed a gene test for spinocerebellar ataxia (SCA) (SCA1, 2, 3, 6, 7, and 17) and dentatorubral-pallidoluysian atrophy (DRPLA).<sup>6</sup> Those with improved clinical symptoms (determined by treating physicians) after treatment with levodopa for >3 months were defined as the positive levodopa response group.

### Standard Protocol Approvals, Registrations, and Patient Consents

The study design was approved by the Institutional Review Board of Seoul National University Hospital (H-1907-100-1048), and the need for obtaining informed consent was waived due to the retrospective nature of the study.

### PET Image Acquisition

As a clinical routine protocol, patients underwent PET/CT imaging after 185 MBq (5 mCi) of [ $^{18}\text{F}$ ]FP-CIT was injected intravenously to patients, and PET/CT was performed 120 minutes after injection with dedicated PET/CT scanners (Biograph true point with true V or Biograph mCT40 or Biograph mCT64, Siemens Healthcare, Erlangen, Germany). A low-dose CT scan (120 kVp, 50 mA) was performed first for attenuation correction and anatomic localization. PET images were reconstructed by an iterative algorithm (ordered-subset expectation maximization) with 21 subsets and 6 iterations. Images were reconstructed with same matrix size with 400 × 400. A 4-mm gaussian post-reconstruction filter was applied.

### Image Preprocessing and Calculation of Binding Ratio

All PET images were spatially normalized into an in-house [ $^{18}\text{F}$ ]FP-CIT PET template.<sup>7</sup> Spatial normalization was performed with statistical parametric mapping software (SPM8, University College of London, UK). Additional gaussian smoothing with full width at half-maximum of 10 mm was implemented to suppress noise and to blur over minor anatomic differences and registration errors. Voxel counts were changed to the binding ratio (BR), defined as  $BR = C_{\text{specific}} / C_{\text{nonspecific}}$ , where C represents PET counts. Mean counts of the occipital cortex were regarded as nonspecific binding,  $C_{\text{nonspecific}}$ . Automated Anatomical Labeling was used for predefined volumes of interest to define the occipital cortex and striatum. The matrix size of spatially normalized PET images was 91 × 109 × 91, and the voxel size was 2.0 × 2.0 × 2.0 mm<sup>3</sup>. The BR of the putamen and caudate was obtained by predefined Automated Anatomical Labeling volumes of interest.

**Table** Demographic and Clinical Features of Patients With MSA

	Total MSA	MSA-P	MSA-C	<i>p</i> Value
No. (%)	65	42 (65)	23 (35)	
Age, mean (SD), y	63.7 (9.3)	64.0 (10.0)	63.0 (7.9)	0.74
Sex, M/F, n	30/35	19/23	11/12	0.78
Motor onset age, mean (SD), y	61.9 (9.5)	62.0 (10.1)	61.7 (8.3)	0.81
Parkinsonism, n (%)	49/65 (75)	42/42 (100)	7/23 (30)	<0.0001
Cerebellar symptom, n (%)	26/65 (40)	3/42 (7)	23/23 (100)	<0.0001
Urinary incontinence, n (%)	43/65 (66)	25/42 (60)	18/23 (78)	0.14
Orthostatic hypotension, <sup>a</sup> n (%)	18/65 (28)	14/42 (33)	4/23 (17)	0.13
Positive levodopa response, n (%)	12/42 (29)	12/41 (29)	0/1 (0)	0.12
Duration from motor onset to [ <sup>18</sup> F]FP-CIT PET, mean (SD), y	2.1 (1.8)	2.3 (1.9)	1.8 (1.8)	0.32
Mean follow-up duration, mo	34.0 (28.8)	39.1 (31.4)	23.9 (20.6)	0.043

Abbreviations: [<sup>18</sup>F]FP-CIT = [<sup>18</sup>F]fluoro-propyl-carbomethoxy-iodophenyl-tropane; MSA = multiple system atrophy; MSA-C = cerebellar dysfunction-dominant MSA; MSA-P = parkinsonism-dominant MSA.

<sup>a</sup> Orthostatic hypotension with systolic blood pressure drop >30 mm Hg or diastolic blood pressure drop >15 mm Hg within 3 minutes on standing.

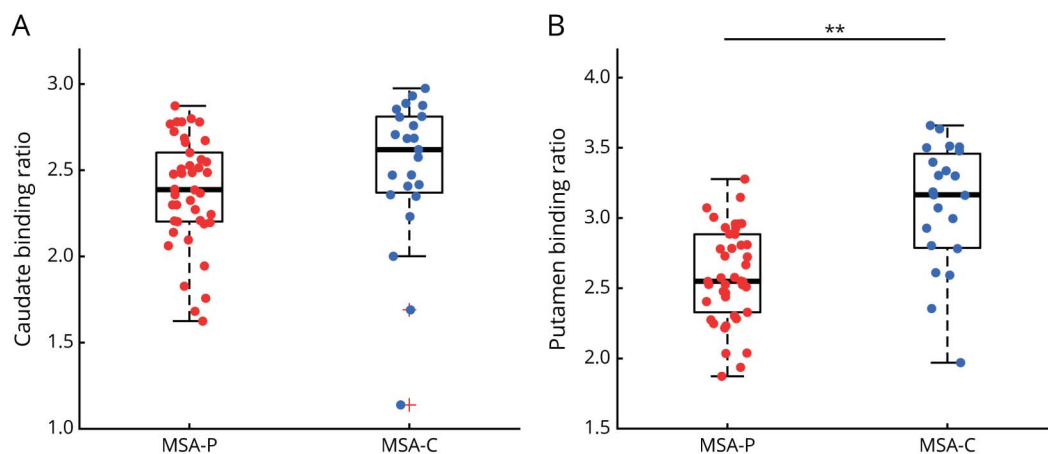
### Voxel-Wise Analysis With a Data-Driven Approach

Principal component (PC) analysis was applied for data dimension reduction. All spatially normalized [<sup>18</sup>F]FP-CIT PET data were changed to a matrix  $M_{ij}$ , where  $i$  is the number of patients and  $j$  is the number of voxels of the brain. PCs were computed from the singular value decomposition of the matrix. The matrix was centered by subtracting the mean image and then decomposed into  $n$  components:  $M = USV^T$ . PCs are represented by  $SV^T$ , and the contribution of the  $k$ th PC to the  $i$ th patient is represented by  $U(i,k)$ . We extracted 5 PCs

from [<sup>18</sup>F]FP-CIT PET data. PC analysis was adapted from the open-source machine learning library (Scikit learn, version 0.22.1, [scikit-learn.org/stable/](https://scikit-learn.org/stable/)) by using Python programming language (version 3.7.6) and applied to the 65 patient datasets.

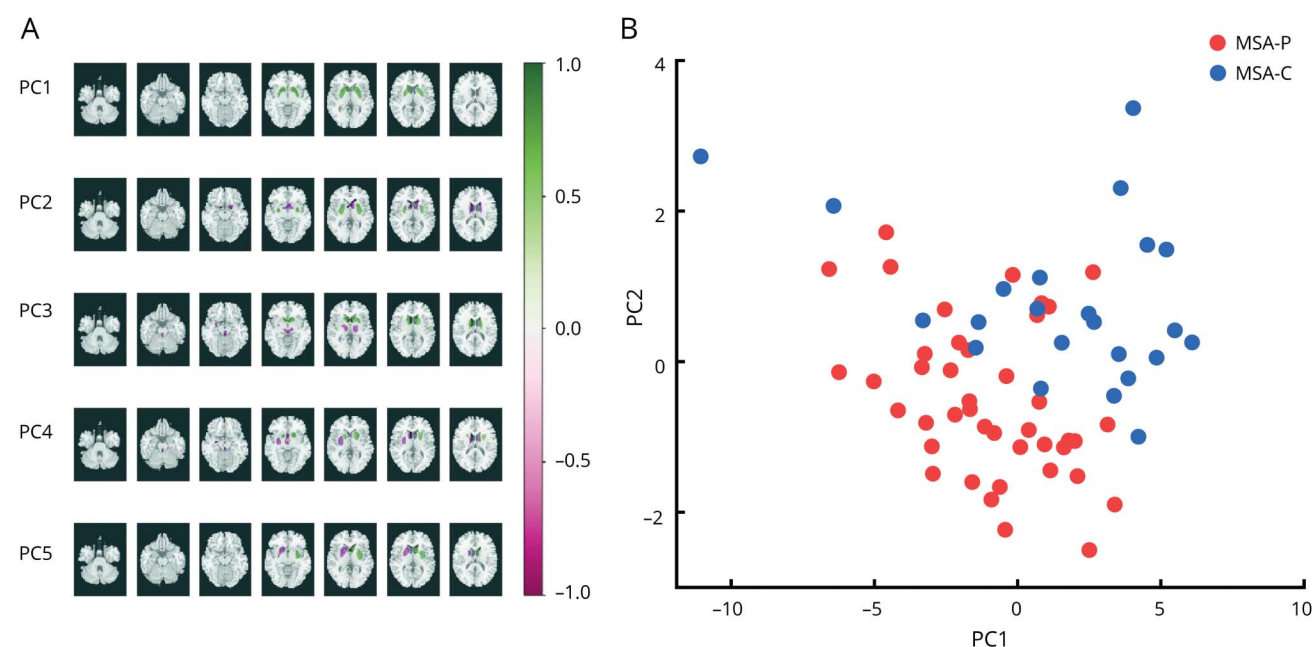
### Statistics

Values are expressed as mean  $\pm$  SD. The Student  $t$  test and  $\chi^2$  test were used to compare continuous variables and categorical variables, respectively, between MSA subtypes. A general linear model was used to compare BRs and PCs across

**Figure 1** Comparison of BR<sub>cau</sub> and BR<sub>put</sub> Between MSA-P and MSA-C

Comparison of binding ratio of caudate nucleus (BR<sub>cau</sub>; A) and binding ratio of putamen (BR<sub>put</sub>; B) between patients with parkinsonism-dominant multiple system atrophy (MSA-P) (red) and cerebellar dysfunction-dominant multiple system atrophy (MSA-C) (blue). Boxplot denotes average as a central line within a box and 25th and 75th percentile values as an outline of a box, and minimum and maximal numbers are marked as error bar with outliers marked separately. General linear model was used to compare principal components between groups with age as a cofactor (\*\* $p < 0.01$ , general linear model with age as a cofactor).

**Figure 2** PCs Derived From Whole-Brain DAT of Patients With MSA-P and MSA-C



(A) Metabolic pattern of dopamine transporter (DAT) binding ratio of total patients with multiple system atrophy (MSA) represented from principal components (PCs) 1 to 5. The z-normalized binding ratio was color-coded as green (increased binding ratio) and purple (decreased binding ratio). (B) Scatterplot of PC1 and PC2 of parkinsonism-dominant MSA (MSA-P) (red) and cerebellar dysfunction-dominant MSA (MSA-C) (blue).

different groups with age as a cofactor. For adjustment of multiple comparison, we used the Benjamini-Hochberg method. The Pearson correlation test was performed to evaluate correlations between the age at onset of motor symptoms and PC values. Data were analyzed with the R program (version 3.4.5, R Foundation for Statistical Computing, Vienna, Austria) and MATLAB (MATLAB R2020a, MathWorks, Natick, MA). Values of  $p < 0.05$  were deemed to be statistically significant.

### Data Availability

The study data are available and will be shared on reasonable request to the corresponding authors.

## Results

### Demographic Features and Conventional Quantification of [ $^{18}\text{F}$ ]FP-CIT PET

A total of 65 patients (35 women, age  $63.7 \pm 9.3$  years, range 40–82 years; 42 with parkinsonian subtype of MSA [MSA-P], 23 with cerebellar subtype of MSA [MSA-C]) were included in the analysis. Patient characteristics are summarized in the table. There were no significant differences in age, sex, onset age, and time from onset to [ $^{18}\text{F}$ ]FP-CIT PET between patients with MSA-P and patients with MSA-C (table). Mean  $\pm$  SD duration of follow up was  $34.0 \pm 28.8$  months with minimum of 3 months. Testing for SCA2, 3, 6, 7, and 17 and DRPLA was done in 31, 28, 16, 14, 26, and 14 patients, respectively, and was all negative. In particular, SCA

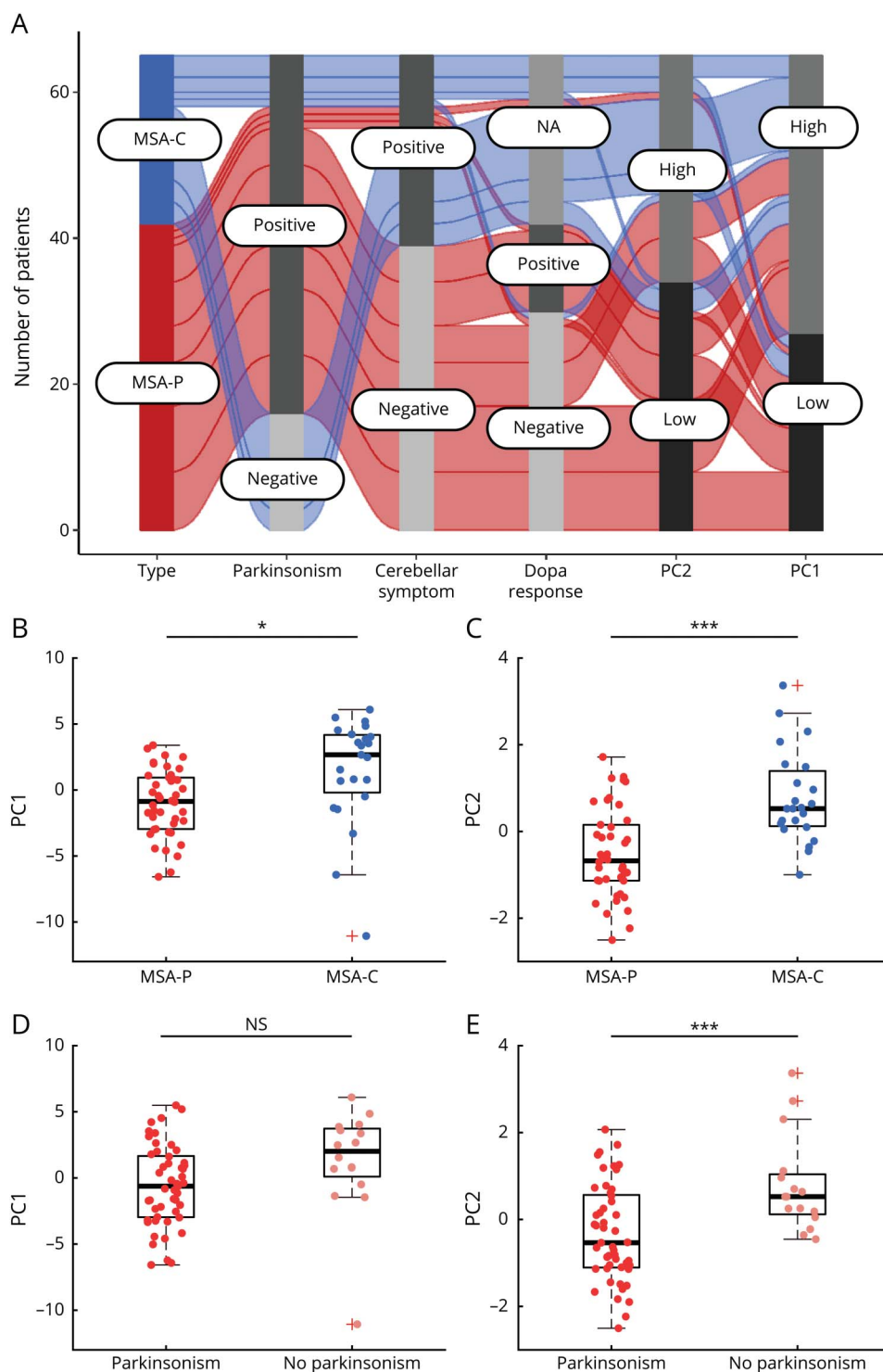
and DRPLA gene test was done in 82.6% (19 of 23) of patients with MSA-C subtype (tested in 16, 14, 13, 12, 17, and 12 patients, respectively). Cerebellar symptoms were positive in 7% of patients with MSA-P, while 30% of patients with MSA-C showed parkinsonism. As a conventional approach, the BR of caudate nucleus ( $\text{BR}_{\text{cau}}$ ) and BR of putamen ( $\text{BR}_{\text{put}}$ ) were compared between patients with MSA-P and MSA-C. There was no significant difference in  $\text{BR}_{\text{cau}}$  between patients with MSA-P and those with MSA-C ( $2.4 \pm 0.3$  vs  $2.5 \pm 0.4$ ,  $p = 0.18$ , corrected  $p = 0.225$ , figure 1A), while the  $\text{BR}_{\text{put}}$  was significantly lower in patients with MSA-P than in patients with MSA-C ( $2.6 \pm 0.4$  vs  $3.0 \pm 0.6$ ,  $p = 0.0013$ , corrected  $p = 0.022$ , figure 1B).

### Spatial Pattern Extraction From [ $^{18}\text{F}$ ]FP-CIT PET of Patients With MSA

We derived the first 5 PCs and their metabolic patterns from the analysis of the spatial patterns of [ $^{18}\text{F}$ ]FP-CIT PET (figure 2A). PC1, PC2, and PC3 explained 70.2%, 9.2%, and 5.5% of the total variance, respectively, thereby explaining >80% of the variance by the combination of PC1 through PC3. Therefore, these 3 PCs were used in the subsequent analysis. Each PC represented a specific pattern of degeneration. PC1 represented a pattern of diffuse [ $^{18}\text{F}$ ]FP-CIT binding of the putamen. A low PC1 value represents a decreased overall DAT binding in the whole putamen. PC2 represented a posterior-dominant decreased [ $^{18}\text{F}$ ]FP-CIT binding of the putamen; thus, a low PC2 value represents the posterior putaminal-dominant



**Figure 3** Comparison of PCs Between Subtypes of Multiple System Atrophy, Parkinsonism



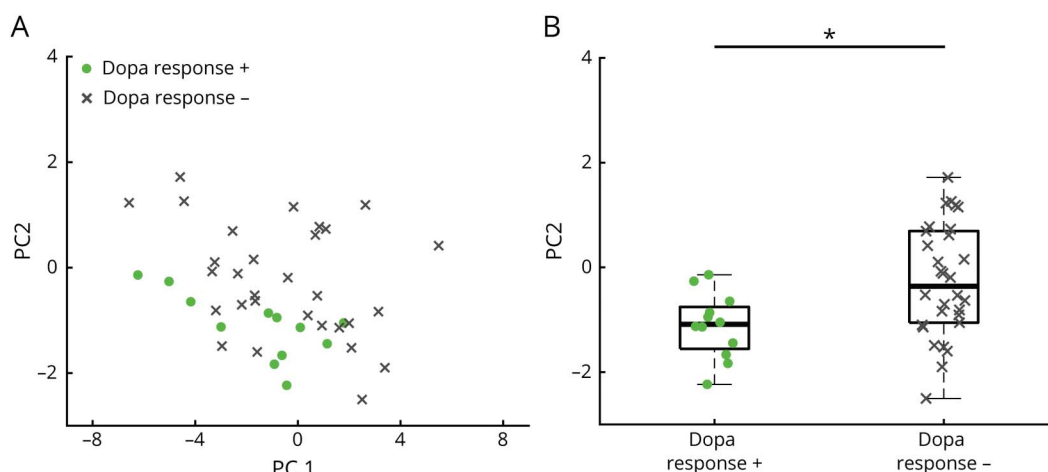
(A) Alluvial diagram showing patients cluster among different variables. Comparison of (B) principal component (PC) 1 and (C) PC2 between patients with parkinsonism-dominant multiple system atrophy (MSA-P) (red) and cerebellar dysfunction-dominant multiple system atrophy (MSA-C) (blue). Boxplot denotes average as a central line within a box and 25th and 75th percentile values as an outline of a box, and minimum and maximal numbers are marked as error bar with outliers marked separately. General linear model was used to compare PCs between groups with age as a co-factor. (D) PC1 and (E) PC2 boxplot shown in the same format as panels B and C with the presence of parkinsonism. NA = not applicable.

degeneration of DAT binding. PC3 was associated with increased [ $^{18}\text{F}$ ]FP-CIT binding of the caudate and decreased binding of dorsal pontine nuclei, periaqueductal gray (PAG), and thalamus (figure 2A). A low PC3 value represents low DAT binding in the caudate and high DAT binding in the dorsal pontine nuclei.

### Spatial Patterns of [ $^{18}\text{F}$ ]FP-CIT PET Associated With Clinical Representations of MSA

The scatterplot of PC1 and PC2 of MSA showed distinct distributions for MSA-P and MSA-C (figure 2B). Accordingly, PET image patterns were represented as distinct clusters according to the MSA subtype, parkinsonism, levodopa

**Figure 4** Comparison of PCs of Patients With MSA With and Without Positive Levodopa Response



(A) Scatterplot of principal component (PC) 1 and PC2 of patients with parkinsonism-dominant multiple system atrophy (MSA) prescribed levodopa showing positive levodopa response (dot) and negative response to levodopa (cross). (B) Significant correlation of PC2 with positive levodopa response.

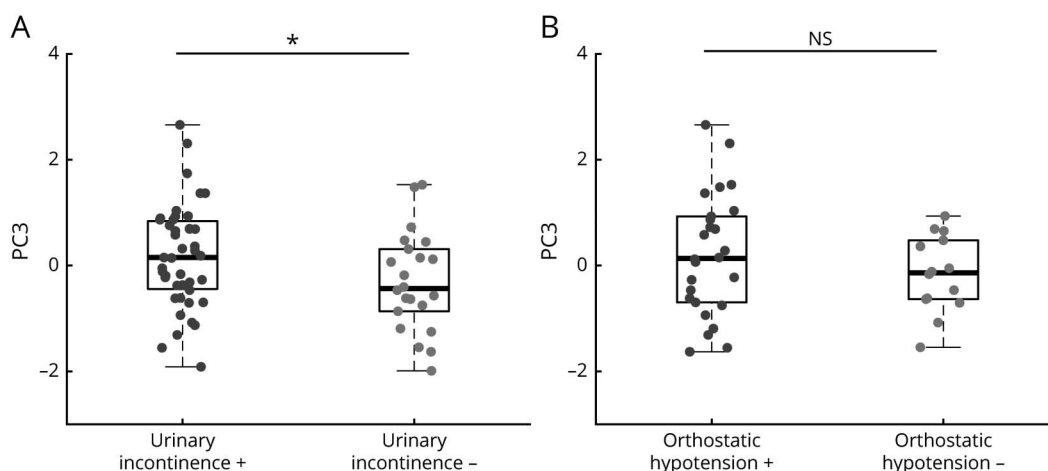
response, and PCs (figure 3A). We found a significant difference between patients with MSA-P and MSA-C in PC1 and PC2 with age as a cofactor ( $-0.8 \pm 2.9$  vs  $1.5 \pm 4.1$ ,  $p = 0.013$ , corrected  $p = 0.022$ , and  $-0.4 \pm 1.2$  vs  $0.8 \pm 1.1$ ,  $p = 5.51 \times 10^{-6}$ , corrected  $p = 2.7 \times 10^{-5}$ , respectively, figure 3, B and C). The decreased PC1 and PC2 suggested the predominant involvement of presynaptic nigrostriatal degeneration in patients with MSA-P. In all patients with MSA, the PC2 was significantly lower in patients with parkinsonism than in those without parkinsonism ( $-0.3 \pm 1.2$  vs  $0.8 \pm 1.1$ ,  $p = 5.34 \times 10^{-5}$ , figure 3E); in contrast, the PC1 showed no significant difference between patients with and without parkinsonism ( $-0.3 \pm 1.2$  vs  $1.3 \pm 4.0$ ,  $p = 0.11$ , figure 3D). Among patients with MSA with parkinsonism, positive levodopa response was associated with PC2

( $-1.1 \pm 0.6$  vs  $-0.1 \pm 1.2$ ,  $p = 0.044$ , figure 4, A and B) but not with PC1 ( $-1.6 \pm 2.5$  vs  $-0.2 \pm 3.2$ ,  $p = 0.21$ ).

The presence of urinary incontinence was associated with higher PC3 with age as a cofactor ( $0.2 \pm 0.9$  vs  $-0.3 \pm 0.9$  with urinary incontinence vs without urinary incontinence, respectively,  $p = 0.036$ , figure 5A) but not with PC1 ( $0.3 \pm 3.2$  vs  $-0.6 \pm 4.1$ ,  $p = 0.35$ ) or PC2 ( $0.1 \pm 1.3$  vs  $-0.2 \pm 1.3$ ,  $p = 0.41$ ). Orthostatic hypotension was not correlated with PC1, PC2, or PC3 (figure 5B).

We also found a significant correlation of lower PC2 with the younger age at onset of motor symptoms in all patients with MSA ( $R = 0.46$ ,  $p = 0.00011$ , figure 6A), and a trend was also

**Figure 5** Correlation of Dopamine Transporter Binding With Autonomic Symptoms



Correlation of principal component 3 (PC3) with the presence of (A) urinary incontinence and (B) orthostatic hypotension (\* $p < 0.05$ , general linear model with age as a cofactor). NS = not significant.

found in both the MSA-P and MSA-C subgroups ( $R = 0.57$ ,  $p = 7.9 \times 10^{-5}$  and  $R = 0.50$ ,  $p = 0.015$ , respectively, figure 6, B and C). Older onset age was correlated with lower PC3 in all patients with MSA ( $R = -0.38$ ,  $p = 0.0017$ , figure 6D), but the correlation was found only in MSA-P ( $R = -0.54$ ,  $p = 0.0002$ , figure 6E), not in MSA-C ( $R = 0.037$ ,  $p = 0.87$ , figure 6F). PC2 and PC3 were not significantly correlated with disease duration (time from onset of symptoms to  $[^{18}\text{F}]\text{FP-CIT}$  image) ( $R = -0.081$ ,  $p = 0.52$  for PC2 and  $R = -0.026$ ,  $p = 0.83$  for PC3). We found no significant correlation of onset age or disease duration with PC1 ( $R = -0.12$ ,  $p = 0.34$  for onset age and  $R = 0.087$ ,  $p = 0.49$  for disease duration).

## Discussion

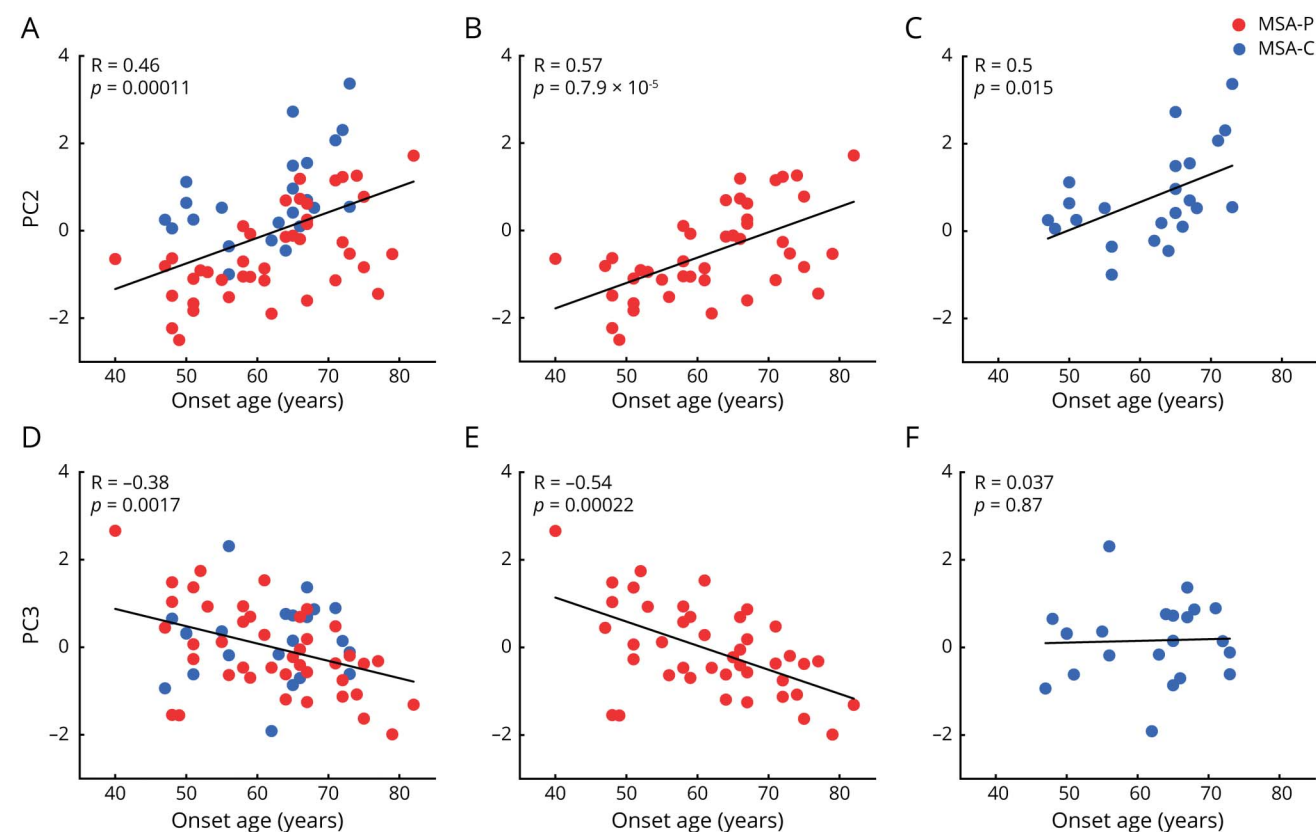
In this study, we examined the whole-brain DAT binding pattern in patients with MSA, which is correlated with clinical variables, including parkinsonism, levodopa response, and autonomic dysfunctions. Furthermore, we found that the DAT binding pattern was related to onset age.

Overall, the DAT binding pattern revealed relatively preserved DAT binding in the striatum in patients with MSA-C, in line with

previous studies.<sup>8,9</sup> A positive levodopa response was significantly correlated with a low PC2 value (posterior-dominant decline) but not with the PC1 value (diffuse decline). Furthermore, PC2, but not PC1, was significantly correlated with parkinsonism in MSA. This result suggests that posterior-dominant loss, rather than diffuse loss, of DAT in the putamen accounts for parkinsonism and its positive levodopa response in MSA. A previous pathologic analysis of 100 patients with MSA showed that those with a good response to levodopa had a preserved anterior part of the putamen, which corresponds to our finding.<sup>10</sup> Patients with MSA usually show a poor response to levodopa therapy,<sup>5</sup> but up to 30% of the patients still show a clinically significant response.<sup>11</sup> Our results suggest that the posterior-dominant dopamine degeneration pattern is a potential predictive factor for the positive levodopa response and that levodopa should be tried, especially in those patients.

We found that PC3 was associated with the presence of urinary incontinence in MSA. A higher PC3 value corresponds to low DAT binding in the dorsal pontine area and PAG matter. Reflex circuitry connections between the lumbosacral spinal cord and dorsal pontine nuclei, including the locus coeruleus, raphe nucleus, and PAG, are responsible for controlling bladder function.<sup>12</sup> In addition, neurons in the rostromedial area (pontine

**Figure 6** Correlation of Dopamine Transporter Binding Pattern With Age at Onset of MSA



Significant correlation of principal component (PC) 2 with older age at onset of (A) total multiple system atrophy (MSA), (B) parkinsonism-dominant MSA (MSA-P), and (C) cerebellar dysfunction-dominant MSA (MSA-C). Correlations between PC3 and age of onset of (D) total MSA, (E) MSA-P, and (F) MSA-C. The  $p$  values were calculated with Pearson correlation analysis.

micturition center) and the PAG play a central role in controlling micturition.<sup>12</sup> Classically, the degeneration of the preganglionic intermediolateral cell column in the spinal cord has been suggested as a pathologic substrate for urinary dysfunction in MSA. However, a series of pathologic studies have failed to find any correlation between neuronal loss in the spinal cord and severity of urinary dysfunction in MSA, which suggests that degeneration in the supraspinal structure as a pathologic correlate of urinary dysfunction in MSA.<sup>13</sup> From this perspective, a previous autopsy study reported that degeneration of the dorsal pontine area and PAG neurons was correlated with urinary dysfunction.<sup>14</sup> Currently, there are not many series of studies showing a correlation between dorsal pontine catecholaminergic degeneration and urinary incontinence in vivo using functional neuroimaging.

The correlation of lower PC2 with younger onset age suggests that patients with MSA with a relatively early onset show more severe posterior putaminal–predominant degeneration of nigrostriatal projections. Notably, PC2 was also significantly correlated with a positive levodopa response. It has repeatedly been reported that a positive levodopa response and levodopa-induced dyskinesia are frequently observed in patients with early-onset MSA.<sup>15,16</sup> In this regard, our findings may provide a clue to the underlying pathomechanism of age-related levodopa responsiveness in MSA.<sup>15</sup>

We observed that the lower PC3 was correlated with older onset age, which suggests that patients with late-onset MSA may show more caudate degeneration with less involvement in dorsal pontine nuclei. DAT binding in the dorsal pontine area represents the degeneration of the dorsal pontine nucleus with noradrenaline/serotonin transporters, including the dorsal raphe, locus coeruleus, and PAG, which are responsible for autonomic dysfunction.<sup>12</sup> Our data show relatively severe degeneration of the dorsal pontine nucleus in patients with relatively early-onset MSA. Thus, our results support a higher prevalence of autonomic dysfunctions in early-onset MSA compared with late-onset MSA.<sup>15</sup>

There are several limitations in the current study. First, this was a retrospective study with a limited number of patients who underwent [<sup>18</sup>F]FP-CIT PET. Because [<sup>18</sup>F]FP-CIT PET is not routinely performed in patients with MSA, there is a possibility of selection bias in that the study population may not reflect the general MSA population. Second, the levodopa response was subjectively defined by the treating physician rather than by the objective monitoring of motor symptoms. Furthermore, whether the positive levodopa response was sustained was not fully investigated. Therefore, we cannot rule out the possibility of placebo in the patients. Third, the patients were not confirmed with autopsy, and we enrolled patients with both probable and possible MSA using clinical diagnostic criteria.<sup>5</sup> However, of note, the patients were followed up for a mean duration of 34 months, and the diagnosis was continuously reappraised at every visit. Future studies with prospective and longitudinal follow-up of patients with MSA with comprehensive evaluations of clinical and cognitive functions as well as DAT imaging are required.

We comprehensively analyzed the spatial patterns of dopaminergic neurodegeneration by using [<sup>18</sup>F]FP-CIT PET among patients with MSA. The pattern of posterior-dominant DAT reduction was associated with the positive levodopa response and parkinsonism symptoms in MSA. Urinary incontinence, which is a core autonomic dysfunction, was associated with decreased DAT binding of the dorsal pontine area. The posterior-dominant decline in DAT binding was associated with a relatively early onset. Our approach to identifying the functional correlates of neuroimaging provides insight into the underlying pathophysiology of a broad spectrum of MSA in terms of clinical phenotypes.

## Study Funding

Supported by the National Research Foundation of Korea grants funded by the Korea government (MSIT) (NRF-2019R1F1A1061412 and NRF-2019K1A3A1A14065446).

## Disclosure

Reeree Lee received travel grant support from Seoul National University Hospital. Jung Hwan Shin received travel grant support from the International Parkinson and Movement Disorder Society and Korean Movement Disorder Society. Hongyoon Choi received research grant support from the National Research Foundation of Korea, Ministry of Health and Welfare of Korea, and Seoul National University Hospital. Han-Joon Kim received travel grant support from the International Parkinson and Movement Disorder Society and Korean Movement Disorder Society and research grant support from the Institute for Information and Communications Technology Promotion, Seoul National University Hospital, New York University, and C-TRI. Gi Jeong Cheon received research grant support from the National Research Foundation of Korea, Ministry of Health and Welfare of Korea, and Seoul National University College of Medicine. Beomseok Jeon received travel grant support from the International Parkinson and Movement Disorder Society and has received research grants support from Peptron and AbbVie Korea. Go to Neurology.org/N for full disclosures.

## Publication History

Received by *Neurology* July 24, 2020. Accepted in final form December 14, 2020.

## Appendix Authors

Name	Location	Contribution
Reeree Lee, MD	Seoul National University Hospital, Korea	Data collection, analysis, and writing of the paper, statistical analysis
Jung Hwan Shin, MD, PhD	Seoul National University Hospital, Korea	Data collection, analysis, and writing of the paper, statistical analysis



**Appendix** (continued)

Name	Location	Contribution
<b>Hongyoon Choi, MD, PhD</b>	Seoul National University Hospital, Korea	Data collection, study design, revisions for intellectual content
<b>Han-Joon Kim, MD, PhD</b>	Seoul National University Hospital, Korea	Data collection, study design, revisions for intellectual content
<b>Gi Jeong Cheon, MD, PhD</b>	Seoul National University Hospital, Korea	Data collection, revisions for intellectual content
<b>Beomseok Jeon, MD, PhD</b>	Seoul National University Hospital, Korea	Data collection, revisions for intellectual content

**References**

1. Wenning GK, Tison F, Ben Shlomo Y, Daniel SE, Quinn NP. Multiple system atrophy: a review of 203 pathologically proven cases. *Mov Disord* 1997;12:133–147.
2. Koch W, Unterrainer M, Xiong G, et al. Extrastriatal binding of [<sup>123</sup>I] FP-CIT in the thalamus and pons: gender and age dependencies assessed in a European multicentre database of healthy controls. 2014;41:1938–1946.
3. Goebel G, Seppi K, Donnemiller E, et al. A novel computer-assisted image analysis of [<sup>123</sup>I]beta-CIT SPECT images improves the diagnostic accuracy of parkinsonian disorders. *Eur J Nucl Med Mol Imaging* 2011;38:702–710.
4. Nicastro N, Garibotto V, Burkhard PR. <sup>123</sup>I-FP-CIT SPECT accurately distinguishes parkinsonian from cerebellar variant of multiple system atrophy. *Clin Nucl Med* 2018;43:e33–e36.
5. Gilman S, Wenning GK, Low PA, et al. Second consensus statement on the diagnosis of multiple system atrophy. *Neurology* 2008;71:670–676.
6. Kim H-J, Jeon BS, Shin J, et al. Should genetic testing for SCAs be included in the diagnostic workup for MSA? 2014;83:1733–1738.
7. Lee JS, Lee DS. Analysis of functional brain images using population-based probabilistic atlas. *Curr Med Imaging Rev* 2005;1:81–87.
8. Bu LL, Liu FT, Jiang CF, et al. Patterns of dopamine transporter imaging in subtypes of multiple system atrophy. *Acta Neurol Scand* 2018;138:170–176.
9. Kim HW, Kim JS, Oh M, et al. Different loss of dopamine transporter according to subtype of multiple system atrophy. *Eur J Nucl Med Mol Imaging* 2016;43:517–525.
10. Ozawa T, Paviour D, Quinn NP, et al. The spectrum of pathological involvement of the striatonigral and olivopontocerebellar systems in multiple system atrophy: clinicopathological correlations. *Brain* 2004;127:2657–2671.
11. Stankovic I, Quinn N, Vignatelli L, et al. A critique of the second consensus criteria for multiple system atrophy. *Mov Disord* 2019;34:975–984.
12. Fowler CJ, Griffiths D, de Groat WC. The neural control of micturition. *Nat Rev Neurosci* 2008;9:453–466.
13. Papp MI, Lantos PL. The distribution of oligodendroglial inclusions in multiple system atrophy and its relevance to clinical symptomatology. *Brain* 1994;117:235–243.
14. Benarroch EE, Schmeichel AM. Depletion of corticotrophin-releasing factor neurons in the pontine micturition area in multiple system atrophy. *Ann Neurol* 2001;50:640–645.
15. Batla A, De Pablo-Fernandez E, Erro R, et al. Young-onset multiple system atrophy: clinical and pathological features. 2018;33:1099–1107.
16. Kim H-J, Jeon BS, Lee J-Y, Yun JY, Kim YE, Paek SH. Young-onset multiple system atrophy. *J Neurol Sci* 2012;319:168–170.